sciendo

**Civil and Environmental Engineering**
**Vol. 17, Issue 2, 597-609, DOI: 10.2478/cee-2021-0060**

# THE BEHAVIOR OF STRIP FOOTING RESTING ON SOIL STRENGTHENED WITH GEOGRID

Duaa AL-JEZNAWI[1,*], Adel A. AL-AZZAWI[1]

[1] Department of Civil Engineering, Al-Nahrain University, Baghdad, Iraq.
[*] corresponding author: duaa.a.al-jezanawi@nahrainuniv.edu.iq

**Abstract**

The soil in Iraq has a low load carrying or bearing capacity and high deflections or settlement because of the applied loads. The use of strip footing as a foundation to support different kinds of heavy structures has become necessary nowadays through solving such problems by using geogrid. This soil improvement technique is widely used all over the world. In this paper, the bearing capacity and settlements were calculated using finite elements and analytical models for strip footing resting on different kinds of soil. The study parameters are footing rigidity, the number of layers in a geogrid, the dimension of geogrid, and spacing of geogrid layers. According to the findings, the geogrid improved the bearing ability of the footing and reduced settlement. The optimum geogrid dimension was three times the footing width, and three geogrid layers were optimum. The changing in footing rigidity also affects the stress and settlement behavior.

**Keywords:**

Finite element;
Strip footing;
Geogrid;
Response;
Soil.

## 1 Introduction

In recent years, the concept of reinforcing soil underneath foundations has become more interesting [1-6]. As the number of appropriate construction sites becomes scarcer, and the demand for poor soil as a base material grows, the use of geogrid reinforcement has become broadly acknowledged [7-9]. The word “reinforced soil” refers to any soil mass whose shear strength has been increased by the addition of resisting parts, such as bars, strips, tubes, grids, or sheets [10]. Different geotechnical engineering applications required reinforcement to increase the performance of the soils. Some scientists have investigated the advantages of soil strengthening in both experimental and theoretical studies [1-6, 11, 12]. During the last decades, several studies have used laboratory model experiments to assess the geogrid-reinforced soil behavior beneath the load of footing [5, 8, 13-17], numerical simulation [16-18], and field experiments [19].

To enhance bearing capacity and minimize expected shallow foundations settlement, both horizontal and vertical reinforcements are included [20]. Geogrids can be an appropriate and low-cost method of increasing bearing or load carrying capacity and decreasing settlements in soils. The increase in soil shear strength which is usually observed with reinforced soil represents a result of displacement of the corresponding soil- strengthening.

Yahia et al. (2016) assess the bearing or load carrying capacity and the deflection of a strip footing lying on sand has poorly graded particles with geogrid reinforcement [20]. This study found that the geogrids improved the curve of the load-settlement for the footing by up to three times the strains at the failure of un-reinforcement sand; in this manner the footing may undergo more elastic settlements before failing with geogrids. In experiments on geogrid strengthened foundations, Abu-Farsakh et al. (2008) and Gill et al. (2013) found that to enhance the bearing capacity ratio, the optimum number of strengthened strata was 3 or 4, and the actual strengthening depth was 1.25 – 2.5 times the width of the foundation [19, 21].

Several scientists have investigated the load carrying or bearing capacity of foundations on strengthened sandy soils in the laboratory [14]. Many aspects, like soil geogrid interface interaction, the number of strengthened strata, strengthening spacing, and the depth of the first strengthening stratum, may impact the behavior of geo-synthetic-reinforced foundations [22].

The bearing capacity of soft soils which have a sand-mat structure was investigated by Park et al. (2013) and discovered that the bearing capacity ratio might be raised by up to 29.4 times based on the configuration of the foundation and the soft soil's initial carrying capacity [23]. The majority of current research focuses on strip foundations or planar-strengthened footings [4]. Makkar et al. (2017) compared bearing capacity enhancement variables using three-dimensional geogrids with rectangular and triangular openings [24]. The improvement in bearing capacity factor was 3.05 for a rectangular opening and 2.7 for a triangular opening.

Das and Omar (1994) investigated the impact of footing breadth, and the findings presented that the ratio of bearing capacity of the geogrid-sand structure decreases as footing width increases [25]. California Bearing Ratio achieved a constant value once the footing width was higher than 130 mm to 140 mm.

Chen et al. (2021) presented the outcomes of stress experiments of the scale plate in laboratory on sand strengthened with geogrid [9]. By altering the length of strengthening geogrid strata and their number, each 25 percent of the foundation width apart, the effects of strengthening length and strengthening number of strata on the load-settlement relation of the strengthened soil footing were examined. Laser sources (to highlight the geogrid strengthening) and a digital camera were used to examine the distortions of the strengthening strata and soil beneath strip loading. The geogrid part beneath strip loading was studied using two-dimensional finite difference software that took into account the shape and the dimension of the experimental simulated tests. The load carrying capacity of the strengthened soil footing and its toughness have developed as the strengthening layers length and number have risen, although this situation is more pronounced as the number of strengthening strata has increased.

The literature review that is performed on geogrids soil reinforcement, reveals that the majority of laboratory/numerical studies focused on soil parameters, variations in geogrids content, and variations in footing sizes. Therefore, further study must be carried to study other parameters that may affect the response of rigid or flexible strip foundation setting on reinforced soil with geogrid which is the objective of the existing study.

## 2 Materials and methods

PLAXIS software is confidently used for simulating every geotechnical problem. By using this software, it can be designing and performing an advanced finite element or soil limit equilibrium analyses and the distortion of rock and stability, as well as the interaction of soil-structure, groundwater, and heat transport. Also, it may demonstrate the non-linear and time-dependent attitude of soils via an advanced constitutive model which incorporated in this software. In this software, typical structure and its interaction with the soil, pore pressures of hydrostatic and non-hydrostatic, and work on a variety of projects as well as foundations, excavations, and embankments, mines, tunnels, and dredging can be implemented.

The nonlinear performance of the soil was simulated by the soil model of Mohr-Coulomb, which is a stress-strain relationship of the elastoplastic model. The foundation was considered as elastic plate components with considerable normal stiffness *EA* and flexural rigidity *EI* varied for rigid and flexible response. Interface parts or elements were implemented to show the relation of the base with the soil and the relation of the soil with geogrid. The coarseness of the interface is demonstrated by selecting an appropriate value for the interface strength decreasing factor *Rinner*. This parameter connects the interface strength to the soil strength parameters (cohesion and angle of friction). A typical value of *Rinner* = 0.85 is employed as an interface component between the geogrid and the soil. This component connects the interface resistance to the soil strength. The soil-plate footing interface element was chosen to be rigid (*Rinner* = 1). The soil factors employed in this study are listed in Table 1, the footing and geogrid characteristics are reported in Table 2 which is taken from [9] for verifications.

Table 1: Soil parameters [9].

| | |
|---|---|
| **Unit weight $\gamma$ [kN/m$^3$]** | 15.6 |
| **Elasticity modulus $E_{ref}$ [kN/m$^2$]** | 8000 |
| **Poisson's ratio $v$** | 0.3 |
| **Cohesion $C_{ref}$ [kN/m$^2$]** | 2 |
| **Internal friction angle $\phi$** | 44$^o$ |
| **Dilatancy angle $\psi$** | 14 $^o$ |

Table 2: Footing and geogrid parameters.

| **Parameter** | **Rigid footing (assumed)** | **Flexible footing (assumed)** | **Geogrid [Chen et al (2021)] [9]** |
|---|---|---|---|
| Flexural rigidity *EI* [kN m$^2$/m] | $4 \times 10^6$ | 4000 | - |
| Axial rigidity *EA* [kN /m] | 400000 | 400 | 200 |

The behavior of the footing in a flexible or rigid fashion can be assessed using a dimensionless parameter $K_s$ that incorporates a representative Young's modulus for the soil $E_s$ combined with terms representing the stiffness of the footing in order to determine an equivalent system stiffness. The stiffness parameter $K_s$ is calculated using Equation 1 by Arnold et al (2010) [26]. The stiffness of the system can be classified based on the ranges for $K_s$ given in Table 3.

$$K_s = \frac{1}{12}\left(\frac{E_f}{E_s}\right)\left(\frac{t}{B}\right)^3 , \quad (1)$$

where $K_s$ is the system stiffness, $E_f$ is the footing Young's modulus, $E_s$ is the soil modulus, $t$ is the footing depth and $B$ is the footing width

Table 3: Stiffness limits for foundation system [26].

| **$K_s$ range** | **System stiffness** |
|---|---|
| 0 | Absolutely flexible |
| 0-0.01 | Semi-flexible |
| 0.01-0.1 | Semi- rigid |
| 0.1-infnity | Rigid |

Triangle plane stress elements for soil automatically generated (15 nodes), plate elements for the foundation, and elastic membrane elements to model the geogrid. Fig. 1 illustrates the solved problem geometry. As illustrated in Fig. 1, the boundary conditions of modeled are that the perpendicular borders are free in vertical direction but confined horizontal direction, whereas the horizontal boundary in the lowest part is fixed.

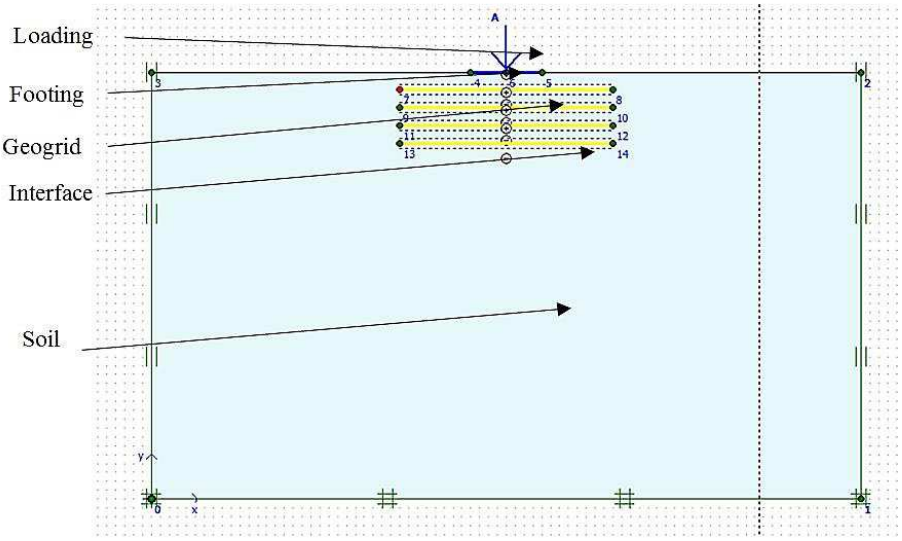



Fig. 1: Soil geogrid simulation with interface.

After the model, geometry has been specified and all clusters and structural objects have been assigned material attributes, the geometry inputs must be separated into finite elements in order to perform the simulation of the problems. The mesh generation of the simulation is presented in Fig. 2.

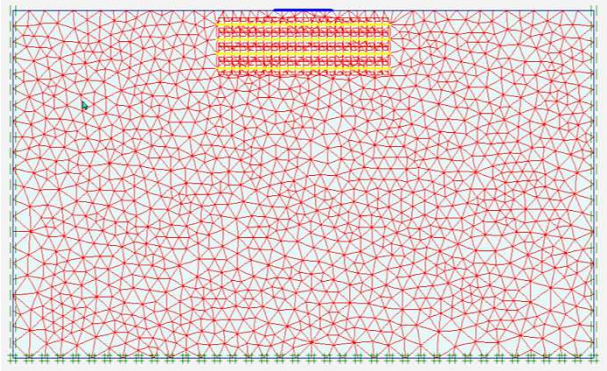


Fig. 2: Finite element mesh.

## 3 Results and discussions

### 3.1 Model verifications

The present study verification example is depended on an already performed study by Chen et al. (2021) [9]. Chen et al. (2021) [9] used a soil tank, a digital camera, a mechanism of loading, and two sources of laser in their experiment. The inside measurements of the tank are 800 x 200 x 590 all dimensions in millimetres (length, breadth, and height). The test box is framed with L-shaped steel beams and has a thickness of 19 mm of toughened glass. Through the glass wall, the soil distortion and reinforcing strata under loading may be seen. A strip footing is modeled using apparatus of a universal testing device and a plate made of steel with 80 mm width and 198 mm length. The footing length was 2 mm smaller than the interior tank breadth that was for minimizing the interaction between the tank and the foundation. The images of the full model foundation were taken using a Canon 550D digital camera has 2592 x 1728 pixels resolution. Light sheets can be generated by laser transmitters to highlight the cross-section target of reinforcements and transparent soils. The sketch of the model test system is presented in Fig. 3.

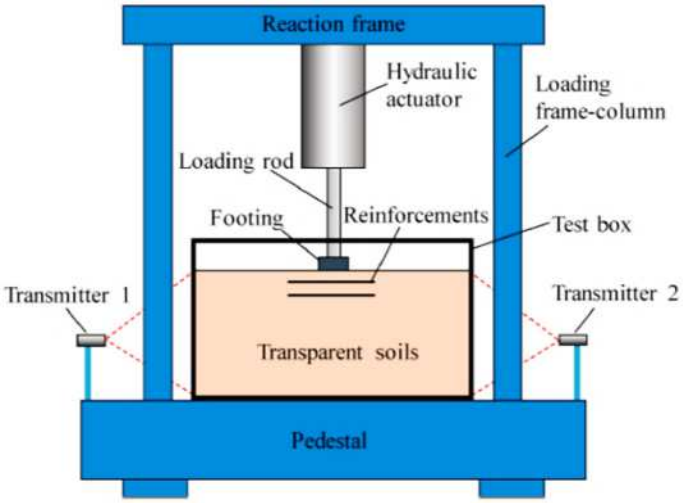



Fig. 3: Testing device [9].

Figs. 4 and 5 show a schematic depiction of the footing model of the geogrid-strengthened. The earth foundation's width was 800 mm and the height was 480 mm. When the height and width of the model are larger than 10 and 6 times the breadth of the foundations, the boundary impact becomes minimal. The influence of the reinforcement length $L = B$, $3B$, and $7B$ and the strengthening layers number $N = 2$, 4, and 6 on the collapse type of strengthened soil footing and the bearing capacity was

investigated in [9] with constant arrangement of geogrid $h/B$ = 0.25 and using of 6 plate load tests (1 is non-strengthened and 5 of them were strengthened geogrid cases).

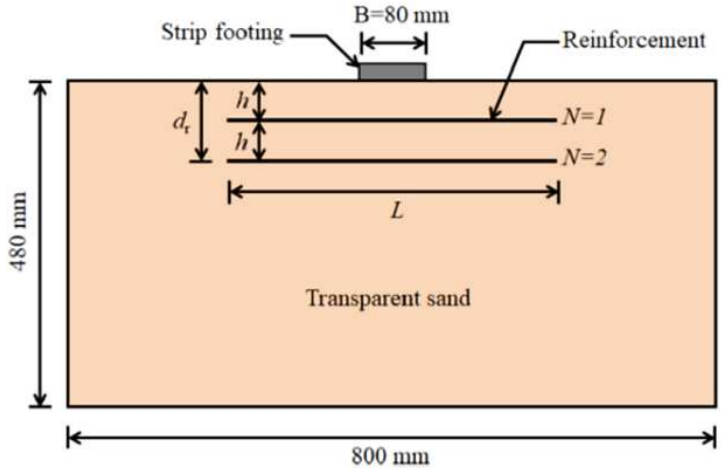



Fig. 4: Graphic view of the strengthened soil footing (consider: the distance in the vertical direction between strengthening strata is $h$, the length of the strengthening is $L$, the number of strengthening strata is $N$, and the overall strengthening depth is $d_r$) [9].

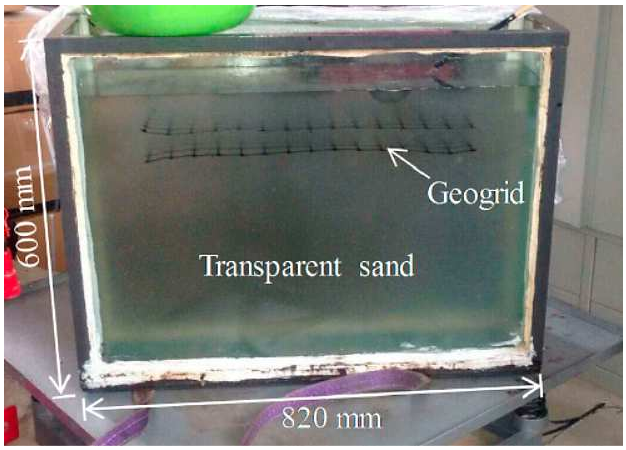



Fig. 5: An image presenting a footing model of a geogrid-reinforced during model preparation [9].

Two cases were selected from the work [9] to make the verification. The first case was rigid footing resting on unreinforced soil. Fig. 6 presents the load-settlement relationship for the existing study finite element and the experimental work [9]. The outcomes reveal good agreement between the two curves.

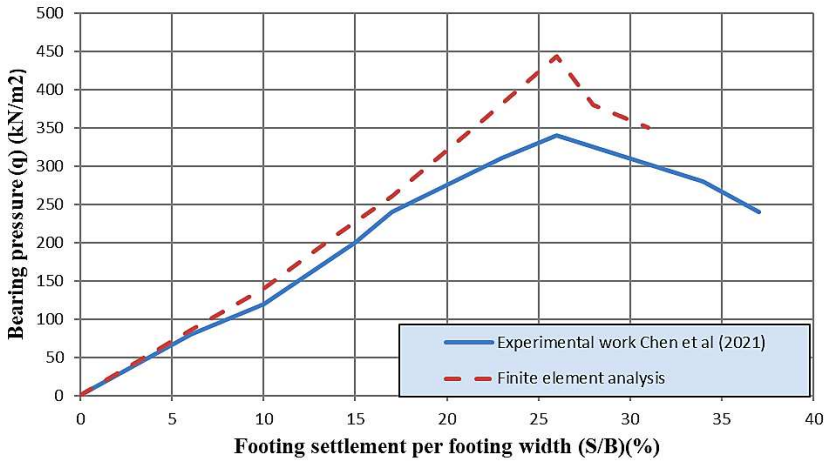



Fig. 6: The curves of the load-settlement for the unreinforced sample.

Meyerhof (1963) [27] presented a way to predict the strip foundation ultimate bearing capacity $q_u$ with the factor of depth $d_f$ as:

$$q_u = C\,N_c d_c + qN_q d_q + 0.5B\gamma N_\gamma d_\gamma\ , \tag{2}$$

where $N_q = e^{\pi \tan\emptyset}\tan^2\left(45+\frac{\emptyset}{2}\right)$, $N_c = \left(N_q - 1\right)\cot\emptyset$, $N_\gamma = \left(N_q - 1\right)\tan(1.4\emptyset)$, (3)

and $d_c$, $d_q$, $d_y$ are the depth factor which equals to 1.

The soil bearing capacity is equal to 380 kN/m$^2$ according to Meyerhof's (1963) equation which is analogous to [9] experimental outcomes and present study finite element outcomes.

Figs. 7, 8, and 9 show the deformed shape, settlement contours, and vertical total stress contours for the present finite element study.

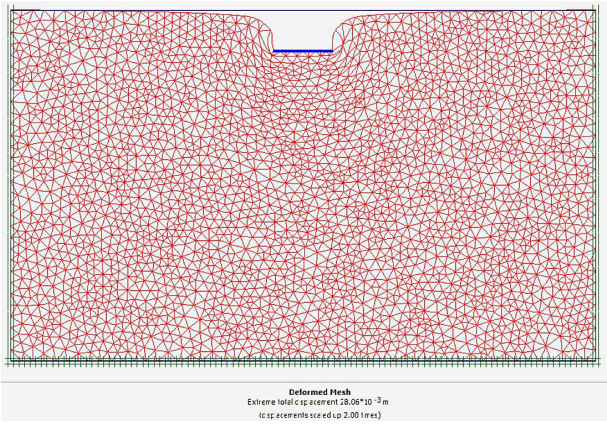



Fig. 7: Deformed shape for rigid strip footing on unreinforced soil.

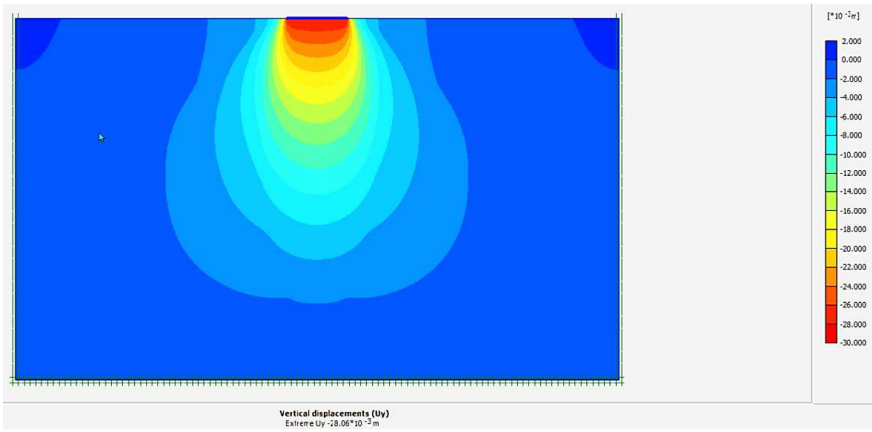



Fig. 8: Settlement contours for rigid strip footing on unreinforced soil.

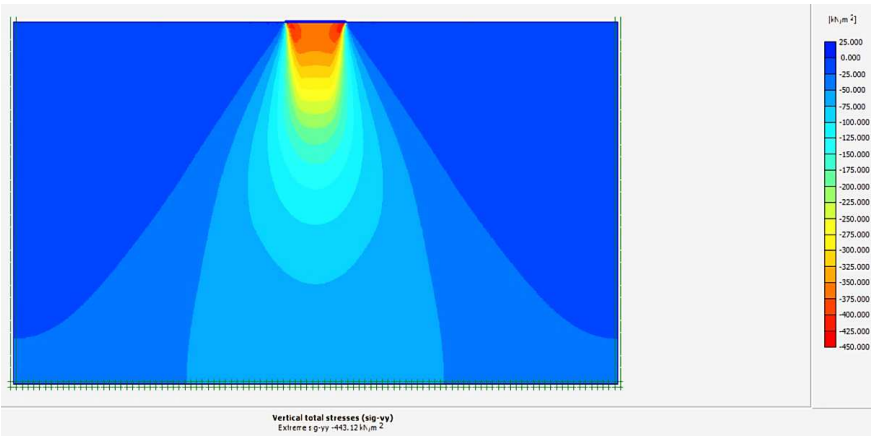



Fig. 9: Vertical stress contours for rigid strip footing on unreinforced soil.

The second verification case was rigid foundation above reinforced soil sample with two geogrid layers. Fig. 10 presents the load settlement relationship for the existing study finite element and the experimental work [9]. The outcomes reveal good agreement between the two curves.

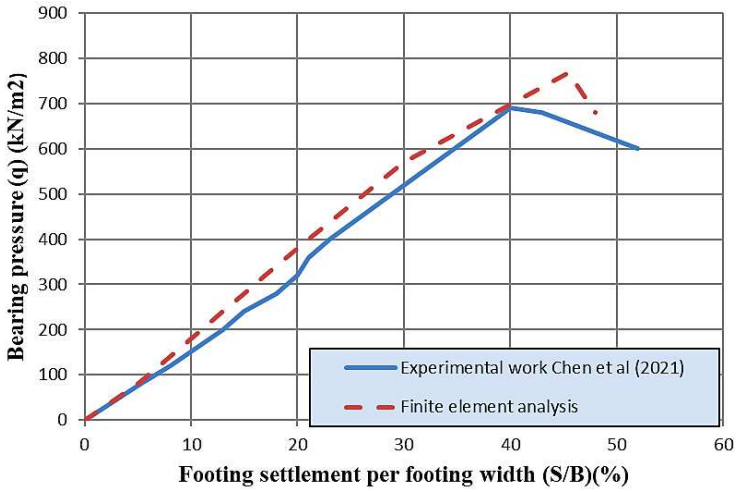



Fig. 10: Load settlement curves for two-layer geogrid reinforced soil.

Figs. 11, 12, and 13 show the deformed shape, settlement contours, and vertical total stress contours for the present finite element study.

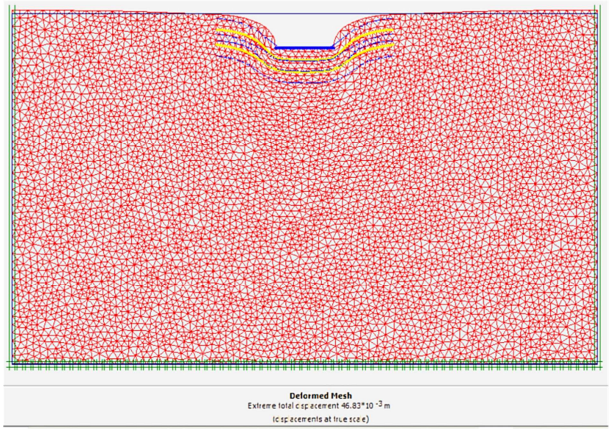



Fig. 11: Deformed shape for rigid strip foundation on two geogrid reinforced soil layers.

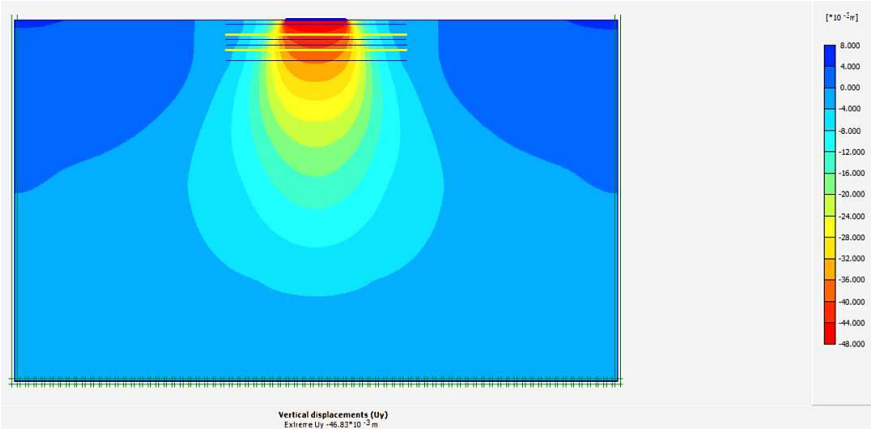



Fig. 12: Settlement contours for rigid strip foundation on two layers geogrid reinforced soil.

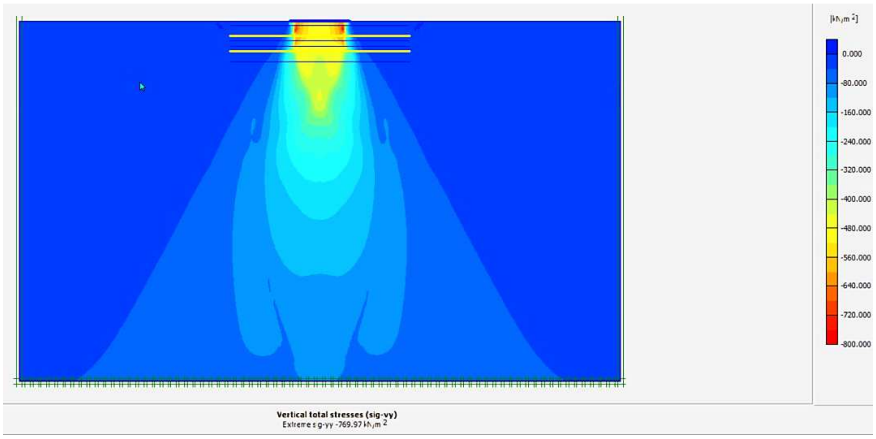



Fig. 13: Vertical stress contours for rigid strip foundation on two layers geogrid reinforced soil.

Fig. 14 shows the comparison between the load settlement curves for rigid strip foundation on un-strengthened and two layers of geogrid reinforced soil. The figure reveals the adequacy of two layers to enhance the soil bearing capacity. The numerical values from Figure 6 and 10 are given in Table 4

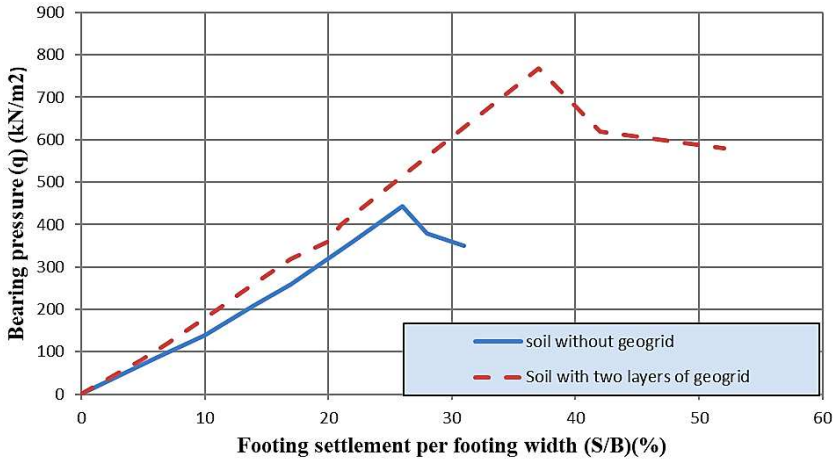



Fig. 14: Load settlement curves for the two layers geogrid reinforced soil.

Table 4: numerical values from Figure 6 and 10.

| | **Maximum bearing pressure [kN/m$^2$] Present study** | **Maximum bearing pressure [kN/m$^2$] Chen et al. (2021) [9]** |
|---|---|---|
| Unreinforced soil | 443 | 340 |
| Reinforced with two geogrids | 769 | 690 |

### 3.2 Parametric study

Several parameters are to be considered in this study:

1) Dimension of geogrid layer,
2) Number of geogrid layers,
3) Distance between geogrid layers,
4) Footing rigidity.

#### 3.2.1 Dimension of geogrid layer *L*

The situation of rigid strip foundation resting on two layers of geogrid strengthened soil tested previously by [9] was considered. The span of the geogrid stratum was varied from *L*/*B*=1, 2, 3, 4 with leaving all other factors fixed. The ratio of the bearing capacity (BCR) is represented the proportion of strengthened soil ($q_{reinforced\ soil}$) to the bearing capacity of un-strengthened soil ($q_{reinforced\ soil}$) and is given by

$$BCR = \frac{q_{reiforced\ soil}}{q_{unreinforced\ soil}} \ . \quad (4)$$

Fig. 15 displays the difference of the ratio of bearing capacity for the rigid strip foundation on two-layer geogrid strengthened soil with geogrid length *L*. The figure illustrates that the BCR becomes higher when the length of the geogrid layer getting longer. As well, this figure illustrates that the amount of increase in BCR decreases extremely after *L*/*B* equal to 3 which indicates the optimal value.

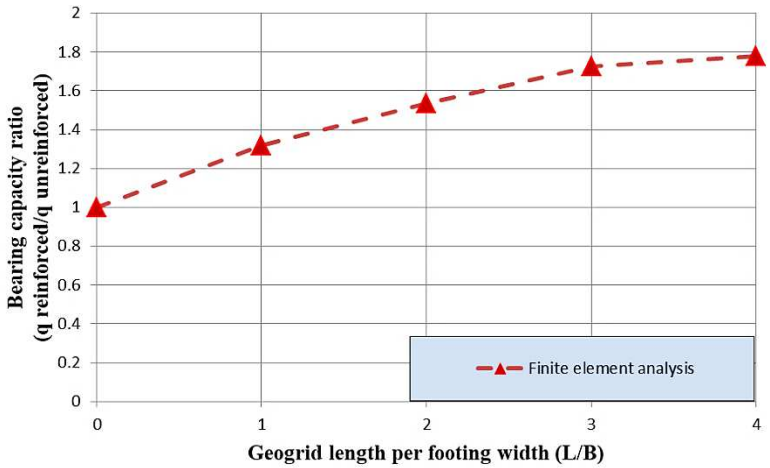



Fig. 15: Difference of bearing capacity ratio for the rigid strip foundation on two layers geogrid reinforced soil.

### 3.2.2 Number of geogrid layers *N*

The case of rigid strip foundation setting on a various number of geogrid layers ranges *N* = 0, 1, 2, 3 and 4. All other parameters are kept constant. Fig. 16 depicts the difference between the rigid strip footing's bearing capacity ratio and the number of geogrid layers *N*. The figures show that the BCR becomes higher when the geogrid layers number become larger. As well as, this figure illustrates that the percentage of increase in BCR decreases extremely after *N* equal to 3 which indicates the optimal value.

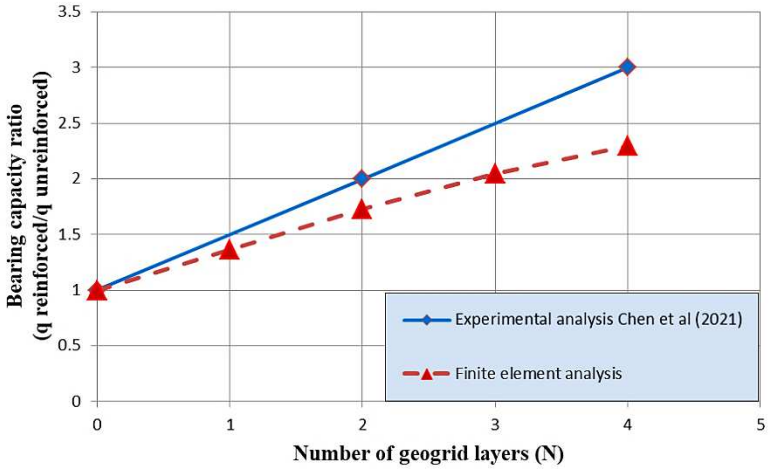



Fig. 16: Difference of bearing capacity ratio for the rigid strip footing with number of geogrid layers.

### 3.2.3 Spacing of geogrid layers *h*

The case of rigid strip footing setting on three layers of geogrid reinforced soil tested previously by [9] was considered. The distance between the geogrid layers was ranged from *h*/*B* = 0.25 and 0.5 keeping all other parameters constant. Figs. 17 and 18 show that the settlement and bearing pressure increases with increasing *h*/*B* from 0.25 to 0.50 which indicates the *h*/*B* = 0.5 is preferred for opening higher load capacity. Fig. 19 illustrates the difference of the geogrid tensile stress with geogrid spacing

*h*. As the geogrid spacing increases from 0.25*B* to 0.5*B* the tensile stresses increase and therefore the geogrid contribution to enhance soil in carrying loads increases.

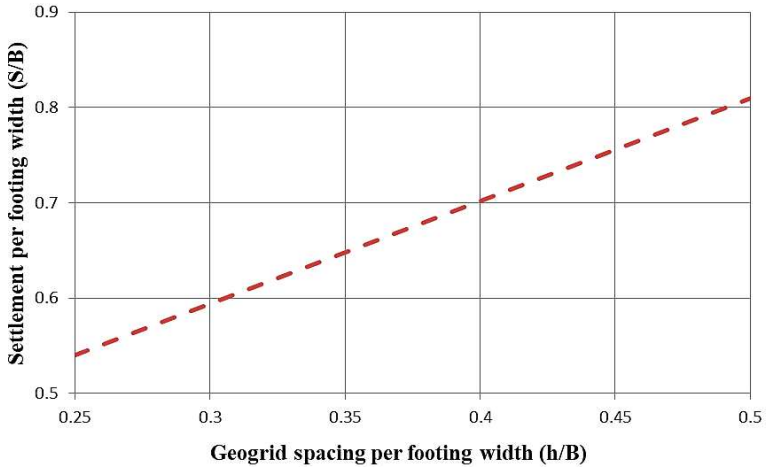



Fig. 17: Variation of the rigid strip footing settlement with geogrid spacing.

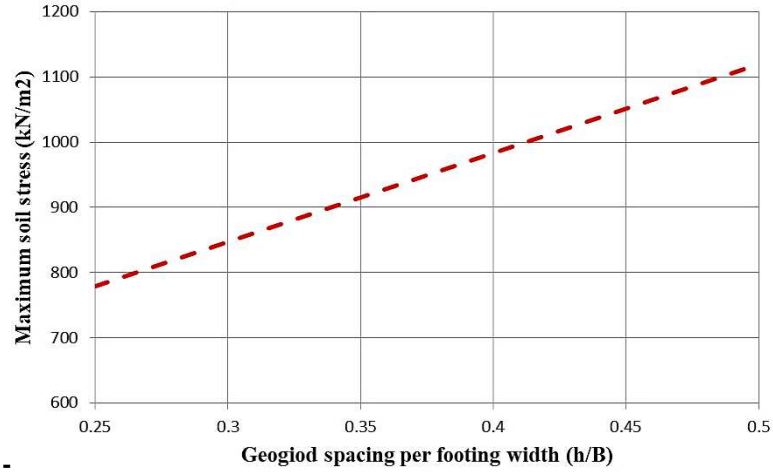



Fig. 18: Variation of the rigid strip footing soil stress with geogrid spacing.

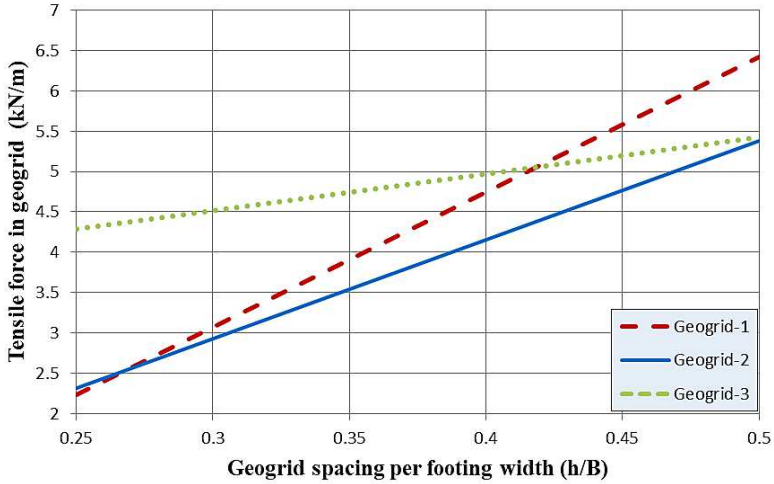



Fig. 19: Variation of the geogrid tensile stress with geogrid spacing.

### 3.2.4 Footing rigidity

The case of rigid or flexible strip footing resting on three layers of geogrid reinforced soil tested previously by [9] was considered. The spacing of the geogrid layer was varied from *h*/*B* = 0.25 to the

geogrid layer length *L*/*B* = 3 keeping all other parameters constant. Figs. 20 and 21 show that the settlement and bearing pressure increases for the flexible footing with almost constant bearing capacity. A stress concentration is visualized near the footing for the flexible case. Fig. 22 illustrates the difference of the geogrid tensile stress with the rigidity of footing, the tensile stresses increase slightly in the geogrid for flexible footing, and therefore the geogrid contribution to enhance soil in carrying loads increases.

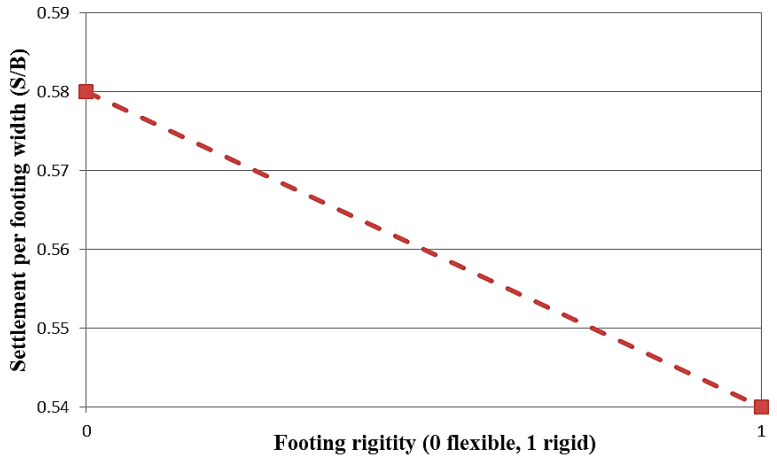



Fig. 20: Variation of the strip footing settlement with footing rigidity.

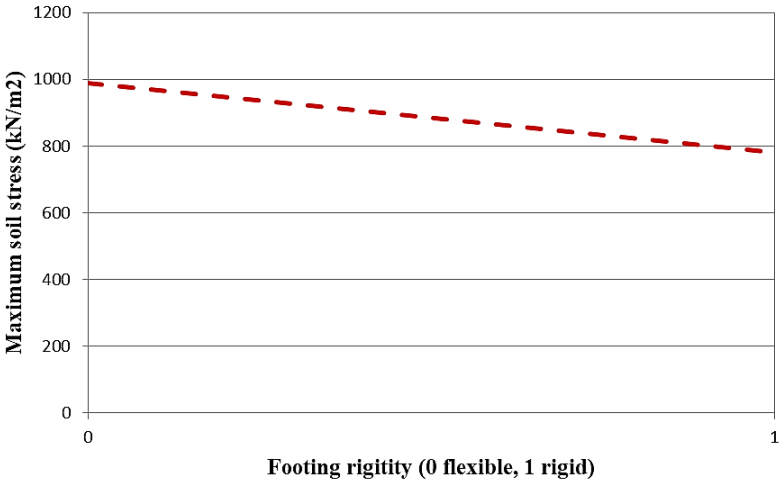



Fig. 21: Variation of the soil stress with footing rigidity.

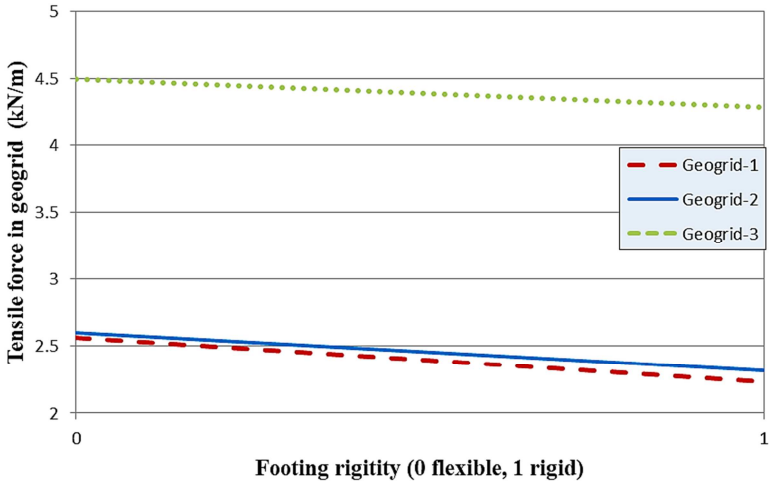



Fig. 22: Variation of the geogrid tensile force with footing rigidity.

## 4 Conclusions

The outcomes from some model tests and numerical simulation revealed that:

- The finite element simulation of the problem reveals good agreement with previous experimental tested strip foundation on geogrid soil.
- The soil bearing capacity of unreinforced soil is equal to 380 kN/m$^2$ according to Meyerhof's (1963) [27] equation which is analogous to the Chen et al. (2021) [9] experimental outcomes and present study finite element outcomes.
- The ratio of bearing capacity (BCR) for the rigid strip foundation on two-layer geogrid strengthened soil increases when the geogrid layer length becomes larger. The proportion of increase in BCR is found to reduce extremely after *L*/*B* equal to 3 which indicates the optimal value.
- When the number of geogrid layers is increased, the ratio of bearing capacity (BCR) for the rigid strip footing increases, but the rate of rise in BCR slows significantly once *N* equals 3, indicating the optimal value.
- For the rigid strip footing resting on three layers of geogrid with layer, the length equals three times the footing width, the settlement and bearing pressure increases with increasing geogrid spacing from 0.25 to 0.50 of footing width which indicates the *h*/*B* = 0.5 is preferred for opening higher load capacity. Also, the variation of the geogrid tensile stress with geogrid spacing *h*. As the geogrid spacing increases from 0.25*B* to 0.5*B* the tensile stresses increase, and therefore the geogrid contribution to enhancing soil in carrying loads increases.
- For the rigid strip footing resting on three layers of geogrid with layer, the length equals three times the footing width and geogrid layer speaking of 0.25 times footing breadth, the settlement and bearing pressure increases for the flexible footing with almost constant bearing capacity. A stress concentration is visualized near the footing for the flexible case. The geogrid tensile stress increases slightly in the geogrid for the flexible footing and therefore the geogrid contribution to enhance soil in carrying loads increases.

## References

[1] BOUSHEHRIAN, J. H. - HATAF, N.: Experimental and numerical investigation of the bearing capacity of model circular and ring footings on reinforced sand. Geotextiles and Geomembranes, 21(4), 2003, pp. 241–256.
[2] DASH, S. - SIREESH, S. - SITHARAM, T.: Model studies on circular footing supported on geocell reinforced sand underlain by soft clay. Geotextiles and Geomembranes, 21(4), 2003, pp. 197–219.
[3] BERA, A. K. - GHOSH, A.: Regression model for bearing capacity of a square footing on reinforced pond ash. Geotextiles and Geomembranes, 23(2), 2005, pp. 261–286.
[4] GHOSH, A. - BERA, A. K.: Bearing capacity of square footing on pond ash reinforced with jute-geotextile. Geotextiles and Geomembranes, 23(2), 2005, pp. 144–173.
[5] PATRA, C. R. - DAS, B. M. - ATALAR, C.: Bearing capacity of embedded strip foundation on geogrid-reinforced sand. Geotextiles and Geo-membranes, 23(5), 2005, pp. 454–462.
[6] PATRA, C. R. - DAS, B. M. - BHOI, M. - SHIN, E. C.: Eccentrically loaded strip foundation on geogrid-reinforced sand. Geotextiles and Geomembranes, 24(4), 2006, pp. 254–259.
[7] ANAND, S. - PRABHULING, U.: Ultimate Load Response of a Square Footing Subjected to Axial and Eccentric Load on Geogrid-Reinforced Soil. Jordan Journal of Civil Engineering, Vol. 15, No. 1, 2021.
[8] LATHA, G. M. - SOMWANSHI, A.: Effect of reinforcement form on the bearing capacity of square footing on sand. Geotext. Geomembranes, 27, 2009, pp. 409–422.
[9] CHEN, J. - XIAOPENG, G. – RUI, S. - SATHIYAMOORTHY, R. - SONG, J. - JIANFENG, X.: Physical and numerical modelling of strip footing on gegrido reinforced transparent sand. Geotextiles and Geomembranes, Vol. 49, Iss. 2, 2021, 2021, pp. 399-412.
[10] TAWFEK, S. A. - RAID, R. A. - ZEYAD, S. M.: Behavior of Geogrids under Strip Footing Resting on Sandy Soil. Asian Academic Research Journal of Multidisciplinary, 2014.
[11] VINOD, P. - BHASKAR, A. B. - SREEHARI, S.: Behaviour of a square model footing on loose sand reinforced with braided coir rope. Geotext. Geomembranes, 27(6), 2009, pp. 464–474.
[12] IŽVOLT, L. – DOBEŠ, P.: Analysis of measuring the deformation resistance of the subgrade surface of a modernised line Považská Teplá – Žilina. Civil and Environmental Engineering, Vol. 16, Iss. 1, 2020, pp. 210-218, doi: 10.2478/cee-2020-0020.
[13] DAS, B. M. - OMAR, M. T.: The effects of foundation width on model tests for the bearing capacity of sand with geo-grid reinforcement. Geotechnical and Geological Engineering, 12(2), 1994, pp. 133-141.

[14] SHIN, E. C. - DAS, B. M. - LEE, E. S. - ATALAR, C.: Bearing capacity of strip foundation on geogrid-reinforced sand. Geotech. Geol., Eng. 20(2), 2002, pp. 169–180.
[15] DASH, S. K. - RAJAGOPAL, K. - KRISHNASWAMY, N. R.: Performance of different geosynthetic reinforcement materials in sand foundations. Geosynth. Int., 11(1), 2004, pp. 35–42.
[16] LATHA, G. M. - SOMWANSHI, A.: Bearing capacity of square footings on geosynthetic reinforced sand. Geotext. Geomembranes, 27, 2009, pp. 281–294.
[17] MARCALIKOVA, Z. - CAJKA, R.: Determination of mechanical properties of fiber reinforced concrete for numerical modelling. Civil and Environmental Engineering, Vol. 16, Iss. 1, 2020, pp. 86-106, doi: 10.2478/cee-2020-0010.
[18] HAMZAH, S. J.: Nonlinear finite element analysis of reinforced and plain concrete haunched beams under torsion. Civil and Environmental Engineering, Vol. 17, Iss. 1, 2021, pp. 229-241, doi: 10.2478/cee-2021-0024.
[19] ABU-FARSAKH, M. - CHEN, Q. M. - SHARMA, R. - ZHANG, X.: Large scale model footing tests on geogrid reinforced footing and marginal embankment soils. Geotech. Test J., 31(5), 2008, pp. 413–423.
[20] YAHIA, E. A. - ASCE, M. - MOHAMMED, Y. A.: The Performance of Strip Footing Resting on Geogrid-Reinforced Dune Sand. Geo-China (ASCE) GSP 261, 2016.
[21] GILL, K. S. - CHOUDHARY, A. K. – JHA, J. N. – SHUKLA, S. K.: Experimental and numerical studies of loaded strip footing resting on reinforced fly ash slope. Geosynthetics International, Vol. 20 Issue 1, 2013, pp. 13-25.
[22] JIA-QUAN, W. - LIANG-LIANG, Z. - JIAN-FENG, X. - YI, T.: Load-settlement response of shallow square footings on geogrid-reinforced sand under cyclic loading. Geotextiles and Geomembranes, Vol. 46, Iss. 5, 2018, pp. 586-596.
[23] PARK, J. B. - PARK, H. S. - KIM, D.: Geosynthetic reinforcement of sand-mat layer above soft ground. Materials, 6(11), 2013, pp. 5314–5334.
[24] MAKKAR, F. M. - CHANDRAKARAN, S. - SANKAR, N.: Behaviour of model square footing resting on sand reinforced with three-dimensional geo-grid. International Journal of Geosynthetics and Ground Engineering, 3(1), 2017, pp. 1-10.
[25] DAS, B. M. - OMAR, M. T.: The effects of foundation width on model tests for the bearing capacity of sand with geo-grid reinforcement. Geotechnical and Geological Engineering, 12(2), 1994, pp. 133- 141.
[26] ARNOLD, A. - LAUE, J. - ESPINOSA, T. - SPRINMAN, S. M.: Centrifuge modelling of the behaviour of flexible raft foundations on clay and sand. Springman, S M, Laue, J & Seward, L (Eds.), Physical Modelling in Geotechnics. Proceedings of the 7th International Conference on Physical Modelling in Geotechnics (ICPMG 2010) held in Zurich. London: Taylor and Francis, pp. 679–684.
[27] MEYERHOF, G.: Some recent research on the bearing capacity of foundations. Can. Geotech. J. 1(1), 1963, pp. 16–26.